XI International Conference on Computational Plasticity. Fundamentals and Applications
COMPLAS XI
E. Oñate, D.R.J. Owen, D. Peric and B. Suárez (Eds)

A COMPUTATIONAL STUDY ON THE OVERLOAD CHARACTERISTIC CURVES OF PROJECTILE PENETRATING METAL OBJECT

DENG QIONG*, FENG LONG, QI WEI

School of Aeronautics, Northwestern Polytechnical University, Xi'an 710072, P.R. China
e-mail: dengqiong24@nwpu.edu.cn

Keywords: Penetration, target plates, over load curve, Lagrange method, Lagrangian-Eulerian coupling algorithm

Abstract: The paper, based on ANSYS/LS-DYNA software, made a computational study on the overload characteristic curves of projectile penetrating metal objects. Adopting Lagrange method, Lagrangian-Eulerian coupling algorithm and SPH method, respectively, simulated the over-load characteristics of projectiles penetrating single-layer steel plates and multi-layer steel and aluminum alloy plates. The results affirmed that the curves agreed well with each other. The curves reached its peak during every penetrating layer and the accelerator peak declined with layers increasing. And the overload value fluctuated around zero during the penetrating interval. The fact, gained from the velocity curves, was that it dropped gradually, however, reached a plateau during the interval, suggesting that the velocity kept constant, and overload value came to zero. The simulation and the experimental results of penetrating the multi-layer aluminum alloy plates were in well accord. Besides, the overload curves shared the same trends with penetrating the multi-layer steel plates.

1 INTRODUCTION

As for studies about penetrating, consulting the references available, no matter experimental and simulation study, mechanism study gained the major focus. Nesterenko et al [1], using the steel-made columned and conical projectiles to penetrate into the targets of Ti–6Al–4V alloy, study the microstructure, and analyzed its effect on the anti-penetration property. Bøvik et al [2-6] and Dey et al [7-9], made a series of computational simulations and experiments to penetrate the Weldox 460 E steel plates systemically, to investigate the size effect. And Bøvik et al [10-11] also made some studies about penetrating the AA5083-H116 and AA6005-T6 plates. Besides, Gupta et al [12-13] focused on the penetrating mechanism changes ascribed from the projectiles' figure, plates' thickness, by using the penetrating experiments of 1100-H12 aluminum alloy plates with thickness below 3mm. The studies concentrated on the distortion mechanism of the targets and the projectile velocities after penetrating, but it would be difficult to get the overload characteristic curves

from the results, especially, the projectile overload curves could be seldom offered in the simulation study.

Based on the actualities, the paper, based on the ANSYS/LS-DYNA code, made studies about the overload characteristic curves by simulating the penetrating steel, aluminum alloy plates with different layers.

2. THE SELECTION OF CONSTITUTIVE MODELS

(1) Projectile

In order to get fine comparisons with experimental results[14], projectiles, which were made of 35CrMnSiA, with weight 3.2 kg，diameter 62 mm, length 215 mm，and its head arc semi-diameter 70 mm，impacted the target plates with the speed 800 m/s.

(2) Target plates

The target plates, were made of 45# steel, with the size of 10 mm×1200mm×1200mm.

(3) Ascertaining material model and parameters

The plastic Kinematic Model in the LS-DYNA code was adopted, with rate enhancement Cowper-Symonds model [15]. Table.1 showed the materials parameters after consulting Hu Changming et al [15].

Table.1: The materials parameters of projectiles and the target plates [15]

Materil	Density /（kg/m3）	Modula /GPa	Yield strength /MPa	Plastical harding modula/GPa	Passion ratio
35CrMnSiA	8.0×103	206	1 275	2.0	0.284
45#steel	7.85×103	200	496	0.5	0.28

3 OVERLOAD CURVES SIMULATIONS DURING PENETRATING

3.1 penetrating the single steel plate with the thickness 10mm

Adopting Lagrange method, Lagrangian-Eulerian coupling algorithm and SPH method in LS-DYNA code, simulated penetrating and got the over-load characteristic curves, in consequence

(1) Lagrange method

Considering the ratio of the target plate to the projectile diameter, and for optimal computation, a relevant axial symmetry model was built with the adoption of 4-node-2D axial symmetry mesh. And the section along the thick direction of the target plate model was divided into 24 meshes, which adopted single point integrals and sandglass control. The chart.1 showed the penetrating model and the local meshes schematically. And plastic

Kinematic model were selected for the projectile and target plate material.

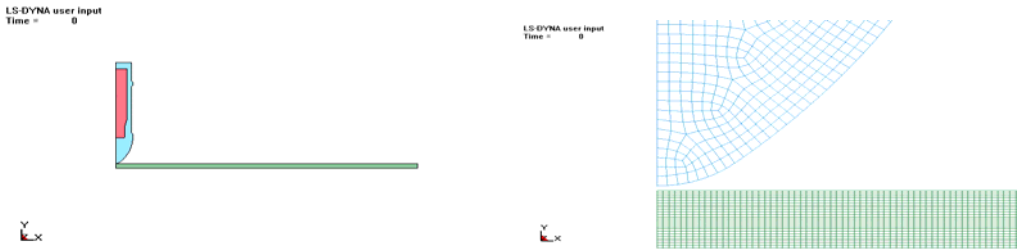

(a) Sketch map of penetrating steel plate (b) Local meshes

Chart 1: Penetrating model and the local meshes of Lagrange method axial symmetry model

The over load curves, gained from computational simulation, was showed in Chart.2, displaying that over load peak reached about 93,000g, and the length of the pulse came to about 60 μs.

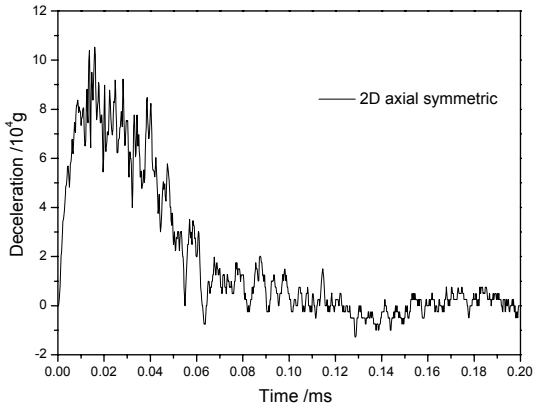

Chart 2 : Overload curves got from Lagrange method axial symmetry model

(2) Lagrangian-Eulerian coupling algorithm

The whole model was divided into single-node integration hex meshes, and a quarter was used to make computing simulation, just for optimal computation. The center section of the target plate was compartmentalized densely into Eulerian finite meshes. Chart.3 gave the schematic of the whole projectile mesh, and the diagram of penetrating the target plate at 120 seconds, respectively.

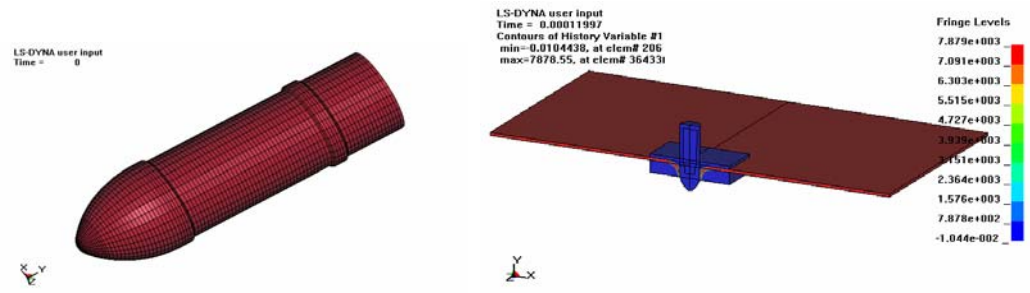

(a) The whole projectile mesh (b) Penetrating the target plate at 120s

Chart 3 : Schematics of penetrating the steel plate using Lagrangian-Eulerian coupling algorithm

And the result of the computational simulations, showed in Chart.4, told that, the overload peak came to 92,000g around, with about 60μs' pulse length.

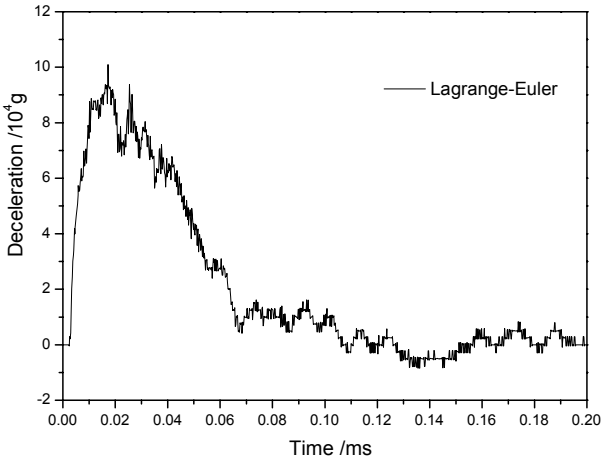

Chart 4 : Overload curve from Lagrangian-Eulerian coupling algorithm

(3) SPH method

The center section of the target plate with the dimension of 100mm×100mm×10mm was defined as SPH particles, with the number of 100×100×10 respectively. The rest were divided by Lagrangian hexahedron mesh. The contact between particles and lagrangian mesh was defined as boundary contact, whereas the contact between particles and projectile was defined as the contact of node to face. The chart 5 showed the schematic of the penetrating process.

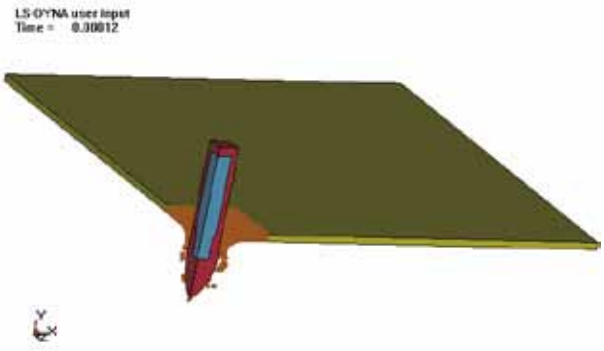

Chart 5 : the penetrating process by SPH method

The overload curve of the simulation, shown as chart 6, revealed the maximum of the acceleration can reached about 90 000, with the pulse length of 60μs around.

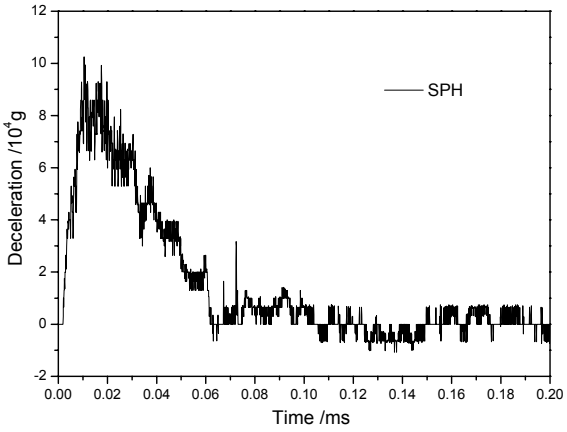

Chart 6 : the overload curve by the SPH method

Comparing with the over-mentioned results, rather difference could be found between the 3 methods. The axial symmetry model have predominated for its rather small computational amount and enough complexity. Thus, the axial symmetry model would be elected in the following simulations.

3.2 The investigation into the overload curves of penetrating multi-layer steel plates

Same to the above-mentioned conditions, over load curves were simulated to investigate into the penetrating into the multi-layer steel plates. The model diagram were shown as Chart 7, with the gap 250 mm, the thickness of 14 mm、10 mm for two layers、three layers steel plates respectively.

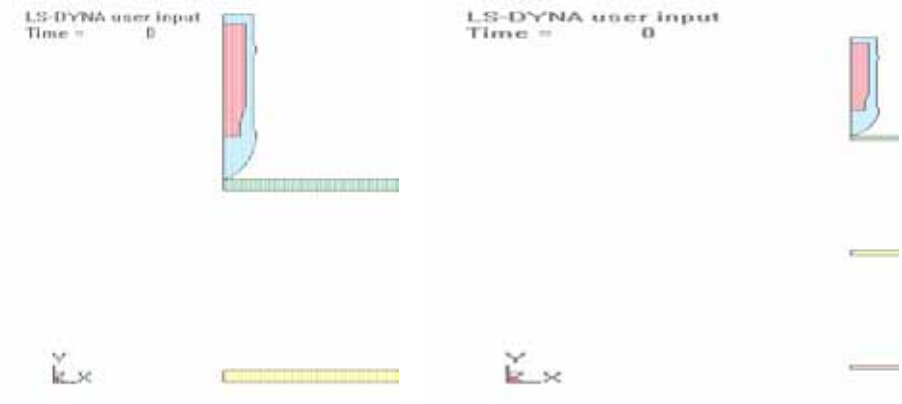

(a) 2 layers steel plates (b) 2 layers steel plates

Cahrt 7 : The model diagram of penetrating multi-layer steel plates

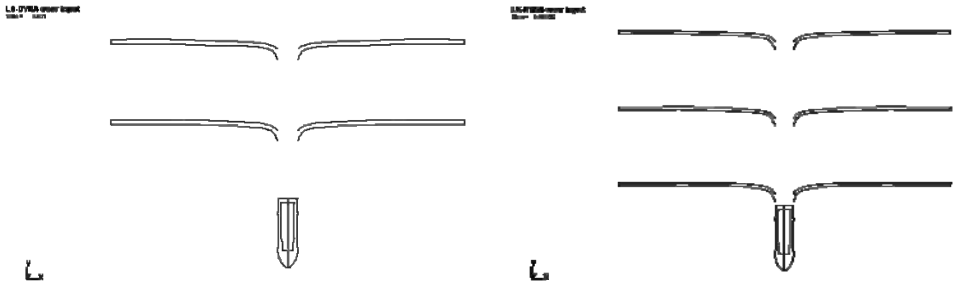

(a) 2 layers steel plates (b) 3 layers steel plates

Chart 8 : The distortion schematic after penetrating multi-layer steel plates

Chart.9 and 10 displayed the overload curves and velocity curves after penetrating two typical plates shown as the above charts.

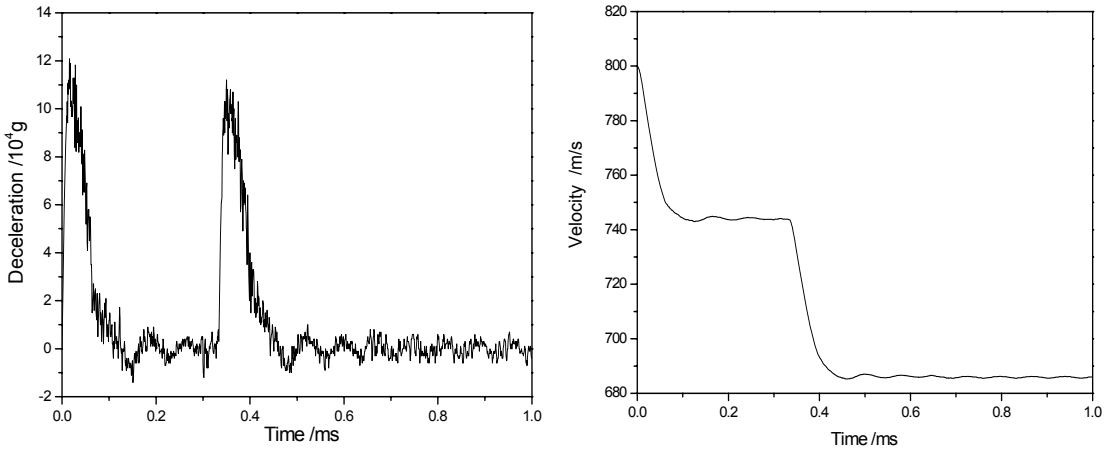

(a) Over load curve (b) Velocity curve

Chart 9 : The over load and velocity curves of penetrating two layers steel plate

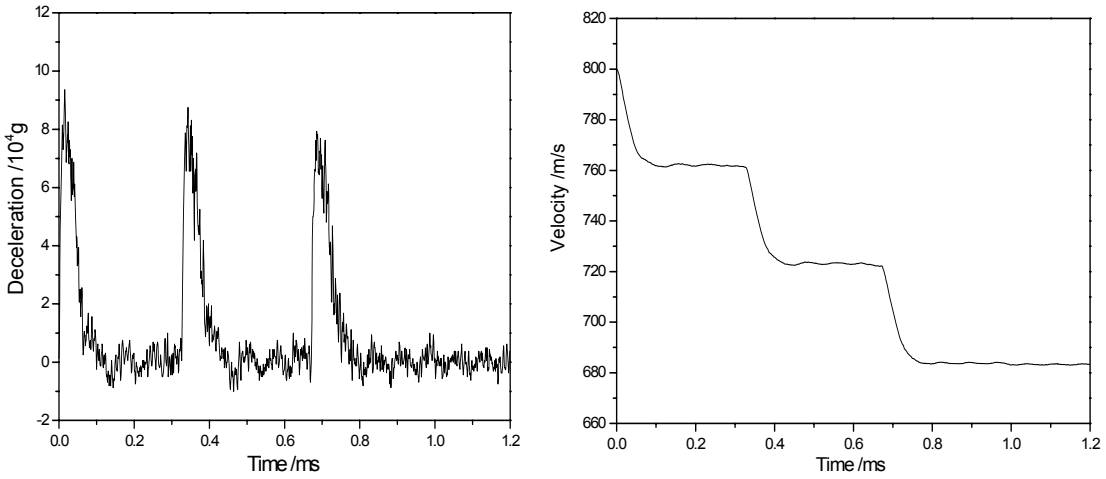

(a) Over load curve (b) Velocity curve

Chart 10 : The over load and velocity curves of penetrating three layers steel plate

The chart.9 and 10 displayed that three distinct peaks could be gained during the penetrating each layer (shown as (a)), and the accelerator sharply descend as the layer increased. During the penetrating interval, the over load fluctuated around zero. Besides, the velocity curve revealed that, during the penetrating each layer, the curve value dropped linearly, whereas during the interval, the value came to a plateau which explained the values kept about constant and the over load value went down towards zero.

3.3 The simulation of penetrating the multi-layer aluminium alloy plates

(1) Establishing model

45# mild steel was elected as the projectile material, and the projectile was modeled with the diameter of 12.7mm, length of 51mm, the mass of 48.5g, and the half ball head. The target plate was modeled as a sandwiched structure, made of the two layers (LY12-CZ, and 2mm in thickness), and foam core (10mm in thickness) sandwiched within the layers. The dimension of the target plate is 300 mm×300 mm×(2 mm+10 mm+2 mm). The Plastic Kinematic Model was elected as the material model for the projectile and the target plate. LY12-CZ was adopted as no strain rate effect. The table 2 showed the material parameters.

Table. 2: Materials parameters

Material	Density / kg/m^3	Modula /GPa	Yield strength /MPa	Plastical harding modula/GPa	Passion ratio
LY12-CZ	2 780	72	345	0.69	0.3
foam	200	0.9	8.3		0.33
45$^{\#}$ steel	7 850	200	496	0.5	0.28

(2) Computational model

As shown as the chart 11, a quarter of the whole model was used for simulation, and the impact section (within the three times of the projectile diameter) was compartmentalized densely in order to ensure the enough accuracy. The rest was divided normally for proper computational amount.

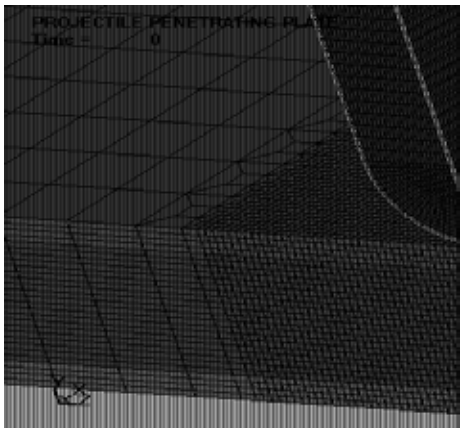

Chart 11 : finite element model of penetrating the aluminum alloy plate

(2) Computational results

The table 3 showed the experimental initial velocity, residual velocity and the computational residual velocity.

Table.3: Comparisons between experimental and\ simulation results of penetrating sandwiched plate/ (m/s)

	Initial velocity	Residual velocity（Exp.）	Residual velocity（Com..）
Sandwiched plate	191.3	169.8	155
	93.4		
	104.5		
	109.2	26.4	32
	73.0		

Abstracted from the table 3, the conclusion was that the simulation velocity went to the experimental velocity very nearly, thus the computational simulation could captured the experiments well.

The accelerator curves and velocity curves were shown as chart 12, gain from the simulation with the initial projectile velocity from 109 m/s, 191 m/s and 250 m/s.

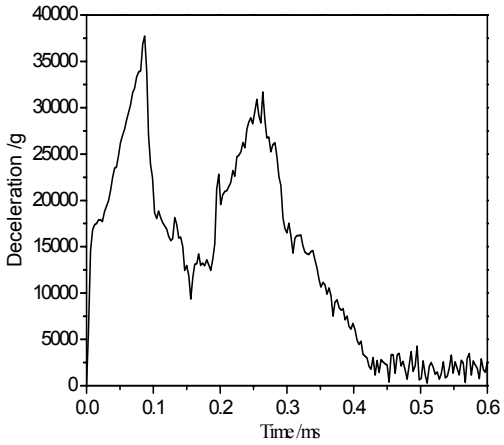

(a) Accelerator curve （v=109m/s）

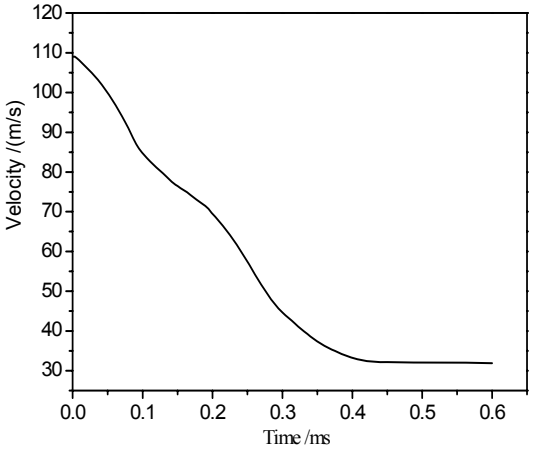

(b) Velocity curve（v=109m/s）

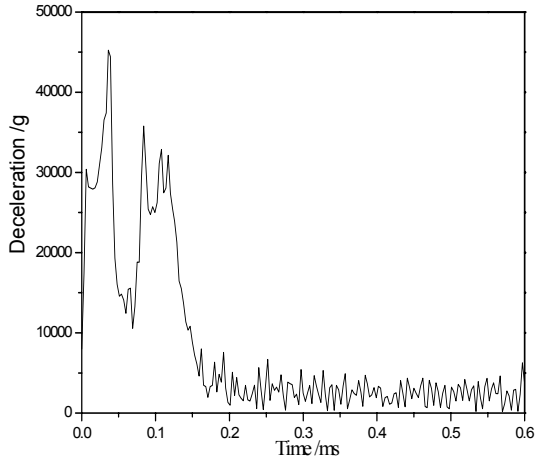

(c) Accelerator curve （v=191m/s）

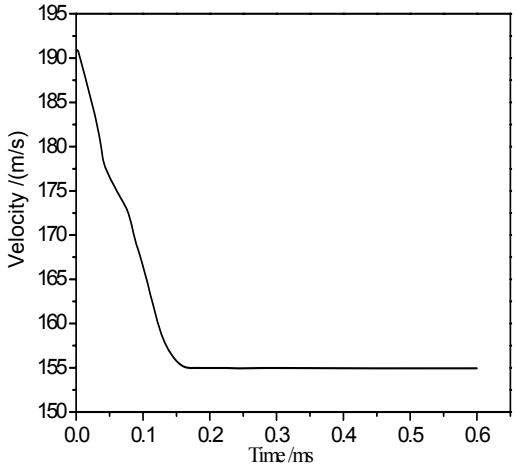

(d) Velocity curve（v=191m/s）

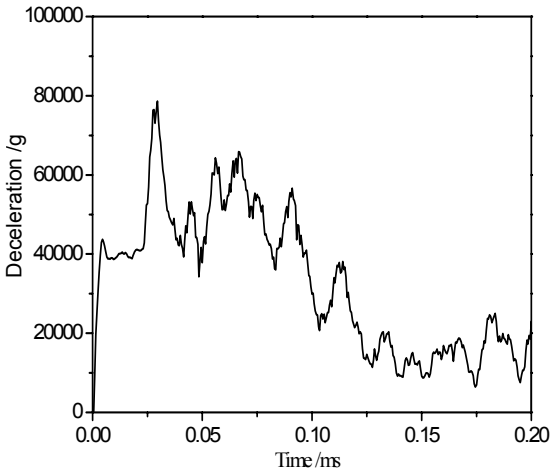

(e) Accelerator curve（v=250m/s）

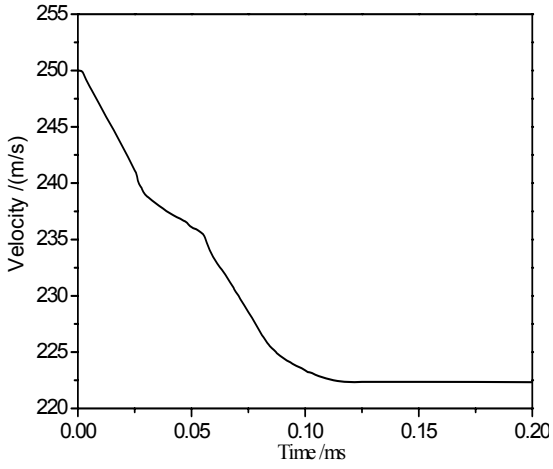

(f) Velocity curve（v=250m/s）

Chart 12 : Model I simulation results

The chart 12 displayed that the over load peaks increased sharply with the initial velocity gaining, resulting in the penetrating time shortening. During the penetrating with the initial velocity of 109 m/s, the accelerator value could reach 38,000g around for the first peak, the second could drop to about 30,000g, and the whole penetrating time could span about 0.44ms. As for the initial velocity of 191 m/s, the accelerator value could reach 45,000g around for the first peak, the second could drop to about 35 000g, and the whole penetrating time could span about 0.18ms. For the initial velocity of 250 m/s, the accelerator value could reach 78,000g around for the first peak, the second could drop to about 62,000g, and the whole penetrating time could span about 0.12ms.

4. CONCLUSION

(1) Based on the Lagrange method, Lagrangian-Eulerian coupling algorithm and SPH method, the computational results were in satisfactorily agreement among them.
(2) Simulating penetrating the multi-layer steel with certain distance, the results explained that the over load value reached its peak within penetrating the each layer, and the accelerator value dropped with the layer increasing. But during the interval, the over load values fluctuated about zero. Abstracted from the velocity curves of penetrating each steel plate, the curve descended linearly, whereas, the curve reached a plateau within the interval, meaning the velocity kept constant, and the over load value went to zero.
(3) Comparing with the experimental and simulation results from penetrating the foam core sandwiched with two layers, the results were in well agreement. The computational overload curve shared the same trend with the penetrating the multi-layer steel plate.

ACKNOWLEDGEMENT

This work was supported by the National Science Foundation of China (grant No. 10872174/A020602).

REFERENCES

[1] Nesterenko V F, Goldsmith W, Indrakanti S S, *et al*. Response of hot isostatically pressed Ti–6Al–4V targets to normal impact by conical and blunt projectiles [J]. International Journal of Impact Engineering, 2003, 28(2): 137–160.

[2] Bøvik T, Langseth M, Hopperstad O S, *et al*. Ballistic penetration of steel plates [J]. Int J Impact Eng, 1999, 22(9-10): 855–886.

[3] Bøvik T, Langseth M, Hopperstad O S, *et al*. Perforation of 12mm thick steel plates by 20mm diameter projectiles with blunt, hemispherical and conical noses, Part I: experimental study [J]. Int J Impact Eng, 2002, 27(1): 19–35.

[4] Bøvik T, Hopperstad O S, Langseth M, *et al*. Effect of target thickness in blunt projectile penetration of Weldox 460 E steel plates [J]. Int J Impact Eng, 2003, 28(4): 413–464.

[5] Bøvik T, Hopperstad O S, Berstad T, *et al*. Numerical simulation of plugging failure in ballistic penetration [J]. Int J Solids Struct, 2001, 38(34–35): 6241–64.

[6] Bøvik T, Hopperstad O S, Berstad T, *et al*. Perforation of 12mm thick steel plates by 20mm diameter projectiles with blunt, hemispherical and conical noses, Part II: numerical simulations [J]. Int J Impact Eng, 2002, 27(1): 37–64.

[7] Dey S, Bøvik T, Hopperstad O S, *et al*. The effect of target strength on the perforation of steel plates using three different projectile nose shapes [J]. International Journal of Impact Engineering, 2004, 30(8-9): 1005–1038.

[8] Dey S, Bøvik T, Hopperstad O S, *et al*. On the influence of fracture criterion in projectile impact of steel plates [J]. Computational Materials Science, 2006, 38(1): 176-191.

[9] Dey S, Bøvik T, Hopperstad O S, *et al*. On the influence of constitutive relation in projectile impact of steel plates [J]. International Journal of Impact Engineering, 2007, 34(3): 464–486.

[10] Bøvik T, Clausen A H, Hopperstad O S, *et al*. Perforation of AA5083-H116 aluminum plates with conical nose steel projectiles—experimental study [J]. Int J Impact Eng, 2004, 30(4): 367–384.

[11] Bøvik T, Clausen A H, Eriksson M, et al. Experimental and numerical study on the perforation of AA6005-T6 panels [J]. International Journal of Impact Engineering, 2005, 32(1-4): 35–64.

[12] Gupta N K, Iqbal M A, Sekhon G S. Experimental and numerical studies on the behavior of thin aluminum plates subjected to impact by blunt- and hemispherical-nosed projectiles [J]. International Journal of Impact Engineering, 2006, 32(12): 1921–1944.

[13] Gupta N K, Iqbal M A, Sekhon G S. Effect of projectile nose shape, impact velocity and target thickness on deformation behavior of aluminum plates [J]. Int. J. Solids. Struct., 2007, 44(10): 3411-3439.